



Investigation of Soft-Tissue Stiffness Alteration in Denervated Human Tissue Using an Ultrasound Indentation System

Mohsen Makhsous, PhD¹⁻⁴; Ganapriya Venkatasubramanian, MS¹; Aditya Chawla, BS¹; Yagna Pathak, BS¹; Michael Priebe, MD⁵; William Z. Rymer, MD, PhD^{2,4}; Fang Lin, DSc^{1,2,4}

¹Departments of Physical Therapy and Human Movement Sciences; ²Physical Medicine and Rehabilitation; ³Orthopaedic Surgery, Northwestern University, Chicago, Illinois; ⁴Sensory Motor Performance Program, Rehabilitation Institute of Chicago, Chicago, Illinois; ⁵Department of Physical Medicine and Rehabilitation, Mayo Clinic, College of Medicine, Rochester, Minnesota

Received December 15, 2006; accepted July 20, 2007

Abstract

Background/Objective: Differences in soft-tissue stiffness may provide for a quantitative assessment and detection technique for pressure ulcers or deep-tissue injury. An ultrasound indentation system may provide a relatively convenient, simple, and noninvasive method for quantitative measurement of changes in soft-tissue stiffness in vivo.

Methods: The Tissue Ultrasound Palpation System (TUPS) was used to quantitatively measure changes in soft-tissue stiffness at different anatomical locations within and between able-bodied persons and individuals with chronic spinal cord injury (SCI). The stiffness of soft tissue was measured at the ischial tuberosity, greater trochanter, posterior mid thigh, and biceps brachii. Additionally, soft-tissue thickness and soft-tissue deformation were also measured.

Results: Significant differences in soft-tissue stiffness were observed within the various anatomical locations tested, in both the able-bodied and SCI groups. Differences in soft-tissue stiffness were also observed between the 2 groups. Participants with SCI had significantly softer tissue in their buttock-thigh area.

Conclusions: TUPS is a clinically feasible technology that can reliably and effectively detect changes in soft-tissue stiffness. The study has provided a better understanding of the tissue mechanical response to external loading, specifically in the SCI population, suggesting the use of tissue stiffness as a parameter to detect and assess pressure-related soft-tissue injury.

J Spinal Cord Med. 2008;31:88-96

Key Words: Spinal cord injuries; Soft-tissue stiffness; Pressure ulcers; Deep-tissue injury; Ultrasound

INTRODUCTION

Nearly 40% of individuals who use wheelchairs develop serious tissue breakdown (1-3) at pressure points due to prolonged sitting or bed rest without proper pressure relief (4,5). Among wheelchair users, individuals with a spinal cord injury (SCI) are particularly susceptible to pressure ulcer formation (6,7). In the population of

persons with SCI, 18.5 to 53.2% develop at least 1 pressure ulcer during their initial acute care and rehabilitation (8), varying with the level and the completeness of the cord injury. Thereafter, from 14.9 to 26.8% of persons with SCI develop a pressure ulcer (8). Notably, pressure ulcers account for approximately 25% of the overall cost of treating patients with SCI, with an estimated annual cost greater than \$1.2 billion (9). They also adversely impact the quality of life of the affected population.

Treatment of established pressure ulcers is extremely difficult, often necessitating expensive, invasive surgeries and postoperative care. A targeted preventive approach is likely to prove less costly and more effective than one focused on treating established pressure ulcers (10,11).

Current documentation and assessment of early pressure ulcer formation and severity are performed

Please address correspondence to Mohsen Makhsous, PhD, Physical Therapy and Human Movement Sciences, Northwestern University, 645 N. Michigan Avenue, Suite 100, Chicago, IL 60640; phone: 312.503.0073; fax: 312.908.0741 (e-mail: m-makhsous2@northwestern.edu).

The project was supported in part by Falk Medical Research Trust and Medical Technology Systems.

© 2008 by the American Paraplegia Society

according to subjective impressions from clinical inspection and palpation with appreciable interobserver inconsistency. Much of the problem with this methodology stems from the frequency with which pressure ulcer formation begins well below the superficial layer of skin as a deep-tissue injury, which has been described by the National Pressure Ulcer Advisory Panel task force (12,13) as the development of significant pressure-related damage under intact skin due to ischemia of the muscle bed and occlusion of the vertical perforating blood vessels (14,15). Full-thickness punch biopsies have shown that lesions that could reasonably be described as Stage I pressure ulcers according to the National Pressure Ulcer Advisory Panel and Agency for Health Care Policy and Research staging systems demonstrate damage to deeper layers (16). These findings indicate that pressure ulcers sometimes start developing deep under the superficial layer of the skin. It is concluded that this kind of deep lesion can not be assessed using the current staging systems (1).

Improved pressure ulcer detection requires a consistent assessment of tissue health. Current diagnostic imaging techniques such as radiography, CT scanning, magnetic resonance imaging (17,18), and B-mode ultrasound mapping (19) can be used to assess tissue health. However, these methods are more expensive and time consuming, and some of them pose potential health risks related to the use of dyes and radiation. One other approach may involve measuring changes in the mechanical properties of soft tissue, which are known to vary between different anatomical sites and demonstrate time dependence, viscoelasticity, and anisotropic behavior (20). Muscle tissue has been observed to be more susceptible to mechanical loading than skin (21, 22). In addition, soft tissue has been reported to have altered thickness and mechanical properties following a compressive load (23), post-SCI (24), and in areas that are injured or adjacent to a pressure ulcer (23,25–27). Therefore, assessing the mechanical properties of soft tissues in areas prone to pressure ulcers may provide important information about the health of those tissues, which could help detect early pressure ulcer formation. One of the simplest interpretations of the mechanical properties is the stiffness of a material, that is, the relationship between load applied to the material and the induced deformation. However, other than elastosonography, the diagnostic imaging methods do not provide information on tissue stiffness, which may be essential for pressure ulcer diagnosis. Therefore, there is a need for an effective and clinically practical diagnostic tool capable of obtaining an indication of tissue stiffness in pressure-ulcer prone areas to quantitatively detect, in an early stage, the pressure ulcer and possibly the deep-tissue injury formation below intact skin.

Among various testing protocols for stiffness of a material, the indentation test is a relatively convenient method, in terms of its simplicity and noninvasive nature,

to determine the stiffness of the skin and subcutaneous tissues *in vivo*.

This study investigated the feasibility of a noninvasive Tissue Ultrasound Palpation System (TUPS) for quantitative measurement of changes in soft-tissue stiffness. TUPS was used to measure the stiffness of soft tissue at the ischial tuberosity (IT), greater trochanter (GT), posterior mid thigh (MT), and biceps brachii (BIC) of able-bodied persons and individuals with SCI. The study presents differences in soft-tissue stiffness within and between groups. The hypotheses were: (a) The differences in soft-tissue stiffness at different body locations can be detected using TUPS, and (b) There are detectable differences on the soft-tissue stiffness between individuals with SCI and able-bodied persons.

MATERIALS AND METHODS

Participants

Participants in this study included 20 able-bodied subjects (33.9 ± 11.4 years, 68.8 ± 9.4 kg, 169.6 ± 6.6 cm, 23.9 ± 2.8 body mass index [BMI], 9 men and 11 women) as the control group and 10 individuals with SCI (33.1 ± 9.0 years, 76.7 ± 16.4 kg, 173.8 ± 7.0 cm, 25.4 ± 5.1 BMI, 8 men and 2 women). Years since injury averaged 8.0 ± 7.4 years, and the participants' level of injury spanned from C6 to T4. The applied experiment protocol was approved by the Institutional Review Board. All ethical principles stated in the Declaration of Helsinki were adhered to while conducting the study.

Sites of Measurement

Tested sites included the IT, GT, MT, and BIC. Data were collected bilaterally from the IT and unilaterally from the GT, MT, and BIC. The mid thigh was on the center line of the posterior side of the thigh at the level of bisecting the lateral femoral epicondyle and the GT. For the BIC, the area of greatest diameter was used.

Tissue Ultrasound Palpation System

The Tissue Ultrasound Palpation System (TUPS) (<http://tups.org>) is a lightweight and portable research device that permits the measurement of the stiffness and thickness (in millimeters) of soft tissues with a pen-size probe, as shown in Figure 1 (fabricated for research not commercial use by Hong Kong Polytechnic University, Hong Kong, China). The hand-held probe contains an A-mode ultrasound transducer at the tip, with a radius of 4.5 mm and an ultrasound frequency of 5 MHz. The ultrasound transducer is both a transmitter and a receiver for ultrasound waves (20), and the echoes received by the transducer can be used to measure the distance between the probe tip and the underlying reflecting surface, which, in current study, was the bone surface. Between the transducer and the handle, a 10-N load cell (ELFS-T3M, Entran Devices, Inc., Fairfield, NJ) (28) measures the force applied to the testing site via the handle. The probe is powered by the main unit, which is

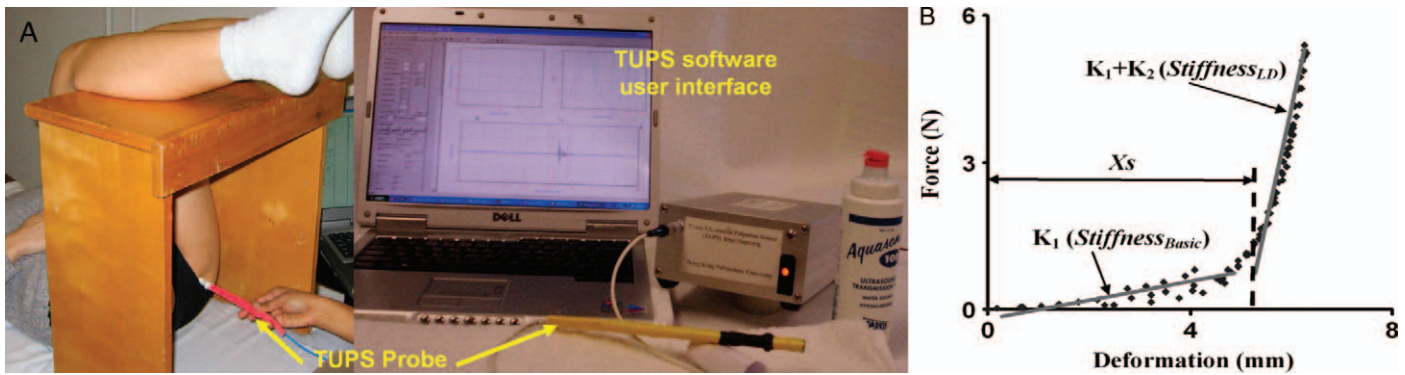


Figure 1. A. Experimental setup. TUPS was used to measure soft-tissue stiffness *in vivo* and noninvasively in a simulated sitting position. The picture shows the testing of the IT on the left side of the subject. **B.** A typical result of TUPS data recorded from the GT of a subject. Also shown are the stiffness parameters of the tested location.

controlled by a personal computer. The software provides real-time information of the ultrasound echoes and off-line data processing.

Data Collection

Participants were asked to lie supine on an examination table and rest their lower legs on a bench to maintain 90° flexion at both the hip and knee joints. This position was intended to simulate the joint configuration of a sitting posture (Figure 1A). After application of the ultrasound gel to the tip, the probe was placed on the skin of the targeted testing location. Tissue was then palpated with alternating loading and unloading cycles to identify a clear echo or signal from the relevant anatomical site. Multiple echoes were visible due to reflection of sound waves off different layers of tissue (eg, skin, fat, muscle). Because the objective was to obtain the gross stiffness of the soft-tissue layer between skin and the bone surface that was composed of skin, fat, and muscles, only the echo reflecting off the bone was of interest to measure the gross thickness of the composite soft-tissue layer. Therefore, attention was paid to the echo that demonstrated the greatest amplitude and maximum displacement during the loading and unloading cycles. Upon finding the correct echo, a minimum of 5 loading and unloading cycles were applied and data were recorded. The data collected were the loading force applied upon the skin surface and the changing thickness of the soft tissue between skin and the underlying bone. The ultrasound echoes were sampled at a frequency of 100 MHz to calculate the thickness of the soft tissue. Then the data of the tissue thickness and the load from the load cell were sampled at 10 Hz. Each trial lasted for 30 seconds and normally contained 5 to 7 loading cycles.

Data Processing

For each recording site, the unloaded thickness of the soft tissue over the underlying bone and underneath the TUPS probe was obtained from the data at the time when the loading force was zero. In addition, in order to

account for the individual variation, this soft-tissue thickness was normalized to the corresponding BMI of each participant. Also obtained from the recording was the maximal deformation (%) of the soft tissue, which corresponded to the maximal loading force (N). The deformation was calculated as the percentage change relative to the initial unloaded thickness at the corresponding site.

For each trial, the recorded loading force and the induced change of soft-tissue thickness from the loading-unloading cycles were used to establish a force-deformation relationship. One such force-deformation relationship is shown in Figure 1B. This relationship was used to estimate the gross stiffness of the composite soft tissue at the tested site.

Initial analysis of the relationship between force applied and deformation in biological soft tissue suggested a nonlinear pattern. However, this nonlinear pattern could be well approximated by 2 connected linear segments with a deflection point (Figure 1B). In light of this, we adopted a model of tissue elasticity composed of 2 parallel springs wherein both springs originated from a common line but 1 spring was a distance x_s (mm) shorter than the other (Figure 2). Following this model, tissue stiffness was gauged in terms of 3 parameters, that is, K_1 (N/mm), K_2 (N/mm), and x_s , in which K_1 and K_2 denoted the stiffness of the 2 springs and x_s was the deformation of the spring K_1 before loading of the spring K_2 . In the recorded data, this x_s corresponded to a tissue deformation before reaching the deflection point (Figure 1B). Mathematically, the relationship for these terms is described by following equations:

$$(1) \quad F = K_1 x \quad x < x_s$$

$$(2) \quad F = K_1 x + K_2 (x - x_s) \quad x_s \leq x < x_{\max}$$

For each trial, the deflection point was first determined for the force-deformation relationship and x_s was obtained. Next, the experimental data with deformation smaller than x_s were fitted to Equation 1 to obtain K_1 .

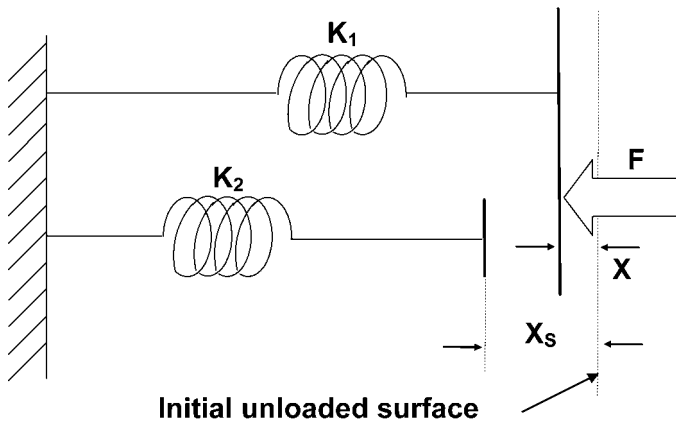


Figure 2. Soft-tissue material model. A soft-tissue model of tissue elasticity based on a system composed of 2 parallel springs (K_1 and K_2 denoted the stiffness of the springs), wherein the system must be deformed a distance x_s before both springs are engaged. The palpating load is represented by F .

Then K_1 was defined as the basic stiffness ($Stiffness_{Basic}$), which represents the slope of the first linear fit of the load-deformation curve (Figure 1B). The rest of the data, which showed deformation larger than x_s , was fitted to Equation 2 to obtain $K_1 + K_2$, which was defined as the large-deformation stiffness ($Stiffness_{LD}$), representing the slope of the second linear fit to the data. The large deformation was achieved by using a higher loading force. An example of this analytical approach is provided in Figure 1B.

Statistical Analysis

A 2-sample t test was performed to detect any significant difference of age, height, weight, and BMI between the control and SCI groups. A paired t test with 2 tails was used to determine any significant difference of the data collected from the left IT and that obtained from the right IT. For each testing location, mean and standard deviation were calculated for $Stiffness_{Basic}$, $Stiffness_{LD}$, x_s , soft-tissue thickness (both absolute and normalized thickness), maximal loading force, and maximal deformation. A two-way analysis of variance was used to find the overall significant effect of group (control and SCI) and location (IT, GT, MT, and BIC). When significance of group effect presented, a 2-sample t test was carried out to obtain the P -value for group effect on each of the locations. When significance of location effect was detected, a paired t test was carried out to obtain the P -value of the location effect within each possible pair of locations within each group. To assess possible gender difference, an additional 2-sample t test was carried out for each of the parameters to compare between all male and female participants. The statistical analysis was performed with SAS software (SAS 9.3, SAS Institute, Gary, NC). The significance level was set to 0.05.

RESULTS

Subject Characteristics

There were no significant differences between the groups for age (33.9 ± 11.4 years for controls vs 33.1 ± 9.0 years for SCI), height (169.6 ± 6.6 cm control vs 173.8 ± 7.0 cm SCI), or BMI (23.9 ± 2.8 control vs 25.4 ± 5.1 SCI). However, the participants in the SCI group had significantly higher body weight than that for the control group (68.8 ± 9.4 kg for controls vs 76.7 ± 16.4 kg for SCI, $P = 0.009$).

Soft-Tissue Thickness

There were no gender differences in our participants for all the recording sites ($P > 0.05$). There was no difference in the soft-tissue thickness collected from the left IT and the right IT ($P > 0.05$). Therefore, for each subject, data from bilateral ITs were averaged to represent the thickness at the IT. Soft-tissue thickness is given as both absolute thickness and normalized thickness (normalized to the BMI) in Table 1 for each recording site for both control and SCI groups. For both groups, the site of the BIC had the thickest soft tissue among all the recording sites, but this finding was only significant in the SCI group and when comparing BIC with GT sites in the control group. Soft tissue over the GT was the thinnest among all sites, and this was significant when compared with that at the MT for the SCI group and the BIC for both groups. There was no difference in the soft-tissue thickness between the 2 groups at all tested locations, except at the BIC, where the SCI group had significantly thicker soft tissue than the control group.

Soft-Tissue Deformation

There was no significant gender difference in the maximal deformation at all recording sites ($P > 0.05$). There was no difference in the maximal deformation collected from the left IT and from the right IT ($P > 0.05$). Therefore, for each subject, data from bilateral ITs were averaged to represent the maximal deformation at the IT. In Table 2, the average maximal deformation achieved during the indentation is reported for each recording site for both groups, together with the average maximal indentation force applied during the loading trials. For both groups, the IT site experienced significantly larger deformation than the other 3 recording sites, except when compared with the BIC in control group. At the same time, the maximal compressive force applied to the IT site was the smallest among all the recording sites. This was significant in control group when compared with all the other 3 locations, but significant in the SCI group only when compared with the BIC.

Soft-Tissue Stiffness

Table 3 summarizes the estimated stiffness of the soft tissue at 4 recording sites for both groups. In control group, both $Stiffness_{Basic}$ and $Stiffness_{LD}$ values were the lowest at the IT site among the 4 locations. $Stiffness_{Basic}$

Table 1. The Absolute Thickness (mean \pm SD; mm) and the Normalized Thickness (mean \pm SD; mm/BMI) of the Composite Soft-Tissue Layer over the IT, GT, MT, and BIC Measured Using TUPS Under No-Load Condition, and the P-Values Obtained from the Statistical Tests

Characteristics	Group, Location							
	Able-Bodied (n = 20)				SCI (n = 10)			
	IT	GT	MT	BIC	IT	GT	MT	BIC
Thickness (mm)	26.59 \pm 0.98	25.41 \pm 1.20	27.18 \pm 1.28	29.34 \pm 1.78	24.11 \pm 1.50	22.16 \pm 1.28	30.53 \pm 2.71	37.23 \pm 1.66
P*	...	> 0.05	> 0.05	> 0.05	...	> 0.05	0.006	< 0.001
P†	> 0.05	0.020	0.005	< 0.001
P‡	> 0.05	> 0.05	0.040
P	> 0.05	> 0.05	> 0.05	0.004
Normalized thickness (mm)	1.13 \pm 0.05	1.07 \pm 0.05	1.15 \pm 0.06	1.24 \pm 0.07	0.98 \pm 0.09	0.89 \pm 0.06	1.24 \pm 0.14	1.49 \pm 0.06
P*	...	> 0.05	> 0.05	> 0.05	...	> 0.05	0.008	0.001
P†	> 0.05	0.017	0.009	0.001
P‡	> 0.05	> 0.05	> 0.05
P	> 0.05	0.024	> 0.05	0.018

Bold type indicates statistical significance.

*Indicates significance for comparison with the value at the IT.

†Indicates significance for comparison with the value at the GT.

‡Indicates significance for comparison with the value at the MT.

||Indicates significance for comparison between the control and SCI groups.

Table 2. The Maximal Force (mean \pm SE; N) Applied to the Soft Tissue over the IT, GT, MT, and BIC Measured Using TUPS

Characteristics	Group, Location							
	Able-bodied (n = 20)				SCI (n = 10)			
	IT	GT	MT	BIC	IT	GT	MT	BIC
Maximal force (N)	3.46 \pm 0.32	5.03 \pm 0.51	4.79 \pm 0.42	5.20 \pm 0.43	2.98 \pm 0.35	4.54 \pm 0.68	3.61 \pm 0.51	4.39 \pm 0.54
P*	...	0.003	0.004	< 0.001	...	> 0.05	> 0.05	0.005
P†	> 0.05	> 0.05	> 0.05	> 0.05
P‡	> 0.05	> 0.05
P	> 0.05	> 0.05	> 0.05	> 0.05
Maximal gross deformation (%)	37.48 \pm 2.55	31.98 \pm 2.71	25.84 \pm 1.37	34.07 \pm 2.73	33.96 \pm 3.04	26.64 \pm 2.44	23.25 \pm 2.31	27.08 \pm 1.64
P*	...	0.014	> 0.001	> 0.05	...	0.011	0.006	0.019
P†	0.020	> 0.05	> 0.05	> 0.05
P‡	0.002	> 0.05
P	> 0.05	> 0.05	> 0.05	0.048

Bold type indicates statistical significance.

*Indicates significance for comparison with the value at the IT.

†Indicates significance for comparison with the value at the GT.

‡Indicates significance for comparison with the value at the MT.

||Indicates significance for comparison between the control and SCI groups.

% Indicates maximal gross deformation under maximal compressive load given as percentage change in thickness over the initial no-load thickness.

Table 3. The Tissue Stiffness (mean ± SE) of the Soft-Tissue Overlaying the IT, GT, and BIC Measured with TUPS

	Group, Location											
	Able-bodied (n = 20)						SCI (n = 10)					
	IT	GT	MT	BIC	IT	GT	MT	IT	GT	MT	BIC	
$Stiffness_{Basic}$ (N/mm)	0.33 ± 0.04	0.45 ± 0.08	0.50 ± 0.05	0.38 ± 0.07	0.23 ± 0.03	0.37 ± 0.07	0.28 ± 0.04	0.23 ± 0.03	0.37 ± 0.07	0.28 ± 0.04	0.36 ± 0.06	
P^*	...	0.037	0.003	> 0.05	...	0.043	> 0.05	...	0.015	> 0.05	0.026	
P^\dagger	> 0.05	> 0.05	> 0.05	> 0.05	> 0.05	
P^\ddagger	> 0.05	> 0.05	
$P^{\ \ }$	0.035	> 0.05	0.001	> 0.05	
$Stiffness_{LD}$ (N/mm)	0.34 ± 0.05	1.01 ± 0.25	0.48 ± 0.06	0.62 ± 0.11	0.32 ± 0.05	1.98 ± 0.65	0.50 ± 0.23	0.32 ± 0.05	1.98 ± 0.65	0.50 ± 0.23	0.23 ± 0.04	
P^*	...	0.009	0.033	0.005	...	0.015	> 0.05	...	0.015	> 0.05	> 0.05	
P^\dagger	0.023	> 0.05	> 0.05	0.007	0.012	
P^\ddagger	> 0.05	> 0.05	
$P^{\ \ }$	> 0.05	> 0.05	> 0.05	0.001	> 0.05	
x_s (mm)	4.79 ± 0.47	4.74 ± 0.53	3.85 ± 0.32	5.17 ± 0.44	4.68 ± 0.37	2.84 ± 0.28	3.74 ± 0.41	4.68 ± 0.37	2.84 ± 0.28	3.74 ± 0.41	4.87 ± 0.34	
P^*	...	> 0.05	> 0.05	> 0.05	...	0.001	> 0.05	...	0.001	> 0.05	> 0.05	
P^\dagger	> 0.05	> 0.05	> 0.05	> 0.05	> 0.05	
P^\ddagger	> 0.05	> 0.05	> 0.05	> 0.05	< 0.001	
$P^{\ \ }$	> 0.05	0.002	> 0.05	> 0.05	> 0.05	0.047	

Bold type indicates statistical significance.
 *Indicates significance for comparison with the value at the IT.
 †Indicates significance for comparison with the value at the GT.
 ‡Indicates significance for comparison with the value at the MT.
 ||Indicates significance for comparison between the control and SCI groups.

was significantly lower at the IT than at the MT ($P = 0.003$) and the GT ($P = 0.037$), whereas $Stiffness_{LD}$ was significantly lower at the IT than at all the other 3 locations (IT vs GT: $P = 0.009$; IT vs MT: $P = 0.033$; IT vs BIC: $P = 0.005$). There was no significant difference in the values of $Stiffness_{Basic}$ and $Stiffness_{LD}$ among the MT, GT, and BIC ($P > 0.05$), except that $Stiffness_{LD}$ at the MT was significantly lower than that at the GT ($P = 0.023$). No significant difference in the value of x_s was found among the 4 locations, except between the MT and BIC, at which x_s at the BIC was significantly larger than that at the MT ($P = 0.024$).

Within the SCI group, data showed that among the 4 locations, $Stiffness_{Basic}$ was the lowest at the IT, but $Stiffness_{LD}$ was lowest at the BIC (Table 3). $Stiffness_{Basic}$ at the IT was significantly lower than that at the GT ($P = 0.043$) and the BIC ($P = 0.026$). $Stiffness_{LD}$ at the GT was the highest among the 4 locations, and the difference was significant (GT vs IT: $P = 0.013$; GT vs MT: $P = 0.007$; GT vs BIC: $P = 0.012$). The x_s value was largest at the BIC, and the value was significantly larger when compared with that at the GT ($P < 0.001$) and MT ($P = 0.047$). The x_s at the IT was also significantly larger than that from the GT ($P < 0.001$).

When comparing the 2 groups, $Stiffness_{Basic}$ at the IT and MT was significantly lower for individuals with SCI (IT: $P = 0.035$; MT: $P = 0.001$). $Stiffness_{LD}$ at the BIC was also significantly lower for the SCI group ($P = 0.001$). The x_s value was significantly lower at the GT ($P = 0.002$) for the SCI group than that for the able-bodied subjects.

DISCUSSION

The incidence and severity of pressure ulcers among individuals with SCI combined with a lack of precise diagnostic measures for monitoring soft-tissue health indicate a need for a quantitative means of objectively documenting or predicting pressure ulcer formation, especially at the earliest stage or even before the skin breakdown occurs. In this study, both the concept of measuring soft-tissue stiffness as a way of appraising tissue integrity and the TUPS device were evaluated. As a first step in this evaluation, TUPS was used to measure tissue stiffness at several anatomical sites on able-bodied participants and participants with SCI.

In both able-bodied persons and individuals with chronic SCI, we found that the soft tissue over the IT was significantly less stiff than at the other 3 locations (GT, MT, and BIC). However, with respect to $Stiffness_{LD}$ values, the BIC was the least stiff among the SCI group. Soft tissue over the GT was among the stiffer ones, especially with respect to $Stiffness_{LD}$. This finding confirmed our hypothesis about the differential stiffness among body locations. The differences of soft-tissue stiffness may be due to the different tissue composition at each location. Tendinous tissue generally has higher stiffness (29); therefore, soft tissue that contains more tendinous tissue tends to be stiffer. For example, more

subcutaneous fatty tissue presents over the location of the IT, whereas more tendinous tissue is usually found at the location of the GT.

Although literature on abnormal tissue mechanical properties is limited, it is established that changes in physiology and sustained external loading can induce an alteration or an adaptation of soft-tissue properties (30–32). Alterations in response to mechanical stress have been observed in human (33–40) and in animal models (41–44), with and without SCI.

Investigation in this study was specifically aimed at finding potential differences in tissue stiffness and thickness, using the evaluated TUPS device, as a result of SCI and tissue denervation. Based on our data, soft-tissue thickness was not significantly different in individuals with SCI compared with able-bodied persons in the areas of the IT, MT, and GT. However, we did find that our participants with SCI had significantly thicker tissue on their arms at the location of the BIC. Upon eliminating the possible gender difference (no gender difference was found for tissue thickness in all participants), we think that the thicker tissue of the BIC seen in the SCI group may come from their more vigorous use of their arms for propelling the wheelchairs.

In addition to the difference in the tissue thickness at the BIC, participants with SCI were found to have significantly softer tissue in their buttock (IT) and thigh (MT) areas. The significantly lower stiffness at the IT in participants with SCI may be attributed to several factors. First, by virtue of having a chronic SCI, the muscular tissue around the IT is denervated and atrophied. Additionally, these participants may possess more fatty tissue in the buttock region from decreased levels of physical activity. Because a softer tissue may indicate an impaired capacity to resist compressive load, this finding may suggest a clue towards the vulnerability of tissue breakdown at the buttock and thigh regions (where the pressure ulcers mostly occur) for those sitting for a prolonged time.

The model used in this study was adapted from a model with similar parallel structure (45), which has been previously used for testing plantar soft-tissue stiffness from individuals with diabetes mellitus and has been proven to be effective.

TUPS data collection was easily performed for both SCI and able-bodied participants. The pen-sized probe and accompanying hardware are both light and compact. Portability was enhanced by installing and running the data collection program from a laptop computer. Data collection took 3 to 5 minutes per anatomical location. Accuracy, reliability, and repeatability of measurements were enhanced by performing at least 3 trials per site, each consisting of multiple loading and unloading cycles. The standard deviation of values at each site was thus minimized.

There are some limitations in our study. The force applied to load the tissue is not constant across the

different trials of data collection because the probe is operated manually to indent the tissue. In addition, the indentation rates are also variable based on how fast the manual indentation is performed. However, it has been shown that the results are relatively insensitive to the indentation rates (28). Probe alignment is also an issue. Although probe misalignment might affect the stress distribution beneath the indenter, the effect on the total force acting on the indenter has been shown to be little for misalignment up to 5° (46). It has been observed that the effect on the indentation response decreased as the thickness increased and became almost negligible when the tissue thickness became larger than double of the indenter diameter. The effects due to misalignment could also be reduced by adopting some amount of preload, which was implemented in our study.

This study presents a novel data-processing methodology for the TUPS. The output of the TUPS has been previously validated for different applications using a linear model (19,28,47–51). However, most of the soft tissue tested in our preliminary studies showed nonlinear behavior. Therefore, a nonlinear material model for the stiffness data for our study was successfully developed and implemented.

CONCLUSION

In summary, the study has not only evaluated the clinical feasibility of a new technology to measure soft-tissue stiffness *in vivo*, but has also provided initial information for a better understanding of the tissue mechanical response to external loading, specifically in an SCI population. Findings of this study provide evidence of the potential utility of using tissue stiffness to detect and assess pressure-related soft-tissue breakdown. Further study is needed, but we believe that the changes in tissue stiffness associated with deep-tissue injury and pressure ulcer formation can reliably and effectively be detected using the TUPS device.

ACKNOWLEDGMENTS

The authors are grateful for technical support from Dr Yongping Zheng in the Department of Health Technology and Informatics, The Hong Kong Polytechnic University, Hong Kong, China.

REFERENCES

1. National Pressure Ulcer Advisory Panel Board of Directors. Pressure Ulcers in America: Prevalence, Incidence, and Implications for the Future: An Executive Summary of the National Pressure Ulcer Advisory Panel Monograph. *Adv Skin Wound Care*. 2001;14(4, part 1 of 2):208–215.
2. Frantz RA. Measuring prevalence and incidence of pressure ulcers. *Adv Wound Care*. 1997;10(1):21–24.
3. Young T. Pressure sores: incidence, risk assessment and prevention. *Br J Nurs*. 1997;6(6):319–322.
4. Barbenel JC. Pressure management. *Prosthet Orthot Int*. 1991;15:225–231.
5. Gawron CL. Risk factors for and prevalence of pressure ulcers among hospitalized patients. *J Wound Ostomy Continence Nurs*. 1994;21(6):232–240.
6. Patterson RP, Cranmer HH, Fisher SV, Engel RR. The impaired response of spinal cord injured individuals to repeated surface pressure loads. *Arch Phys Med Rehabil*. 1993;74(9):947–953.
7. Salzberg CA, Byrne DW, Cayten CG, et al. Predicting and preventing pressure ulcers in adults with paralysis. *Adv Wound Care*. 1998;11:237–246.
8. The National Spinal Cord Injury Statistical Center. *The 2005 Annual Statistical Report for the Model Spinal Cord Injury Care Systems*. Birmingham, AL: University of Alabama; 2005.
9. Salzberg CA, Byrne DW, Cayten CG, van Niewerburgh P, Murphy JG, Viehbeck M. A new pressure ulcer risk assessment scale for individuals with spinal cord injury. *Am J Phys Med Rehabil*. 1996;75(2):96–104.
10. Cervo FA, Cruz AC, Posillico JA. Pressure ulcers: analysis of guidelines for treatment and management. *Geriatrics*. 2000;55:55–60.
11. Whitfield MD, Kaltenthaler EC, Akehurst RL, Walters SJ, Paisley S. How effective are prevention strategies in reducing the prevalence of pressure ulcers? *J Wound Care*. 2000;9(6):261–266.
12. Ankrom MA, Bennett RG, Sprigle S, et al. Pressure-related deep tissue injury under intact skin and the current pressure ulcer staging systems. *Adv Skin Wound Care*. 2005;18(1):35–42.
13. Black JM, Panel N. Moving toward consensus on deep tissue injury and pressure ulcer staging. *Adv Skin Wound Care*. 2005;18(8):415–421.
14. Aronovitch SA. Intraoperatively acquired pressure ulcer prevalence: a national study. *J Wound Ostomy Continence Nurs*. 1999;26(3):130–136.
15. Salcido R, Donofrio JC, Fisher SB, et al. Histopathology of pressure ulcers as a result of sequential computer-controlled pressure sessions in a fuzzy rat model. *Adv Wound Care*. 1994;7(5):23–24.
16. Witkowski JA, Parish LC. Histopathology of the decubitus ulcer. *J Am Acad Dermatol*. 1982;6(6):1014–1021.
17. Bosboom EM, Bouten CV, Oomens CW, Baaijens FP, Nicolay K. Quantifying pressure sore-related muscle damage using high-resolution MRI. *J Appl Physiol*. 2003;95(6):2235–2240.
18. Hincey JY, Vermess M, van Geertruyden HH, Binard JE, Manchepalli S. Magnetic resonance imaging examinations of gluteal decubitus ulcers in spinal cord injury patients. *J Spinal Cord Med*. 1996;19(1):5–8.
19. Wendelken ME, Markowitz L, Patel M, Alvarez OM. Objective, noninvasive, wound assessment using B-mode ultrasonography. *Wounds*. 2003;15(11):351–360.
20. Zheng YP, Mak AF. An ultrasound indentation system for biomechanical properties assessment of soft tissues *in vivo*. *IEEE Trans Biomed Eng*. 1996;43(9):912–917.
21. Daniel RK, Priest DL, Wheatley DC. Etiologic factors in pressure sores: an experimental model. *Arch Phys Med Rehabil*. 1981;62:492–498.
22. Nola GT, Vistnes LM. Differential response of skin and muscle in the experimental production of pressure sores. *Plast Reconstr Surg*. 1980;66:728–733.

23. Gefen A, Gefen N, Linder-Ganz E, Margulies SS. In vivo muscle stiffening under bone compression promotes deep pressure sores. *J Biomech Eng.* 2005;127(3):512–524.
24. Dupont-Versteegden EE, Houle JD, Gurley CM, Peterson CA. Early changes in muscle fiber size and gene expression in response to spinal cord transection and exercise. *Am J Physiol.* 1998;275:C1124–1133.
25. Edsberg LE, Cutway R, Anain S, Natiella JR. Microstructural and mechanical characterization of human tissue at and adjacent to pressure ulcers. *J Rehabil Res Dev.* 2000;37(4):463–471.
26. Linder-Ganz E, Gefen A. Mechanical compression-induced pressure sores in rat hindlimb: muscle stiffness, histology, and computational models. *J Appl Physiol.* 2004;96(6):2034–2049.
27. Bosboom EM, Hesselink MK, Oomens CW, et al. Passive transverse mechanical properties of skeletal muscle under in vivo compression. *J Biomech.* 2001;34(10):1365–1368.
28. Zheng Y, Mak AF. Effective elastic properties for lower limb soft tissues from manual indentation experiment. *IEEE Trans Rehabil Eng.* 1999;7(3):257–267.
29. Fung YC. *Biomechanics: Mechanical Properties of Living Tissue.* 2nd ed. New York: Springer-Verlag; 1993.
30. Duck FA. *Physical Properties of Tissue.* San Diego, CA: Academic Press; 1990.
31. Gao L, Parker KJ, Alam SK, Lernel RM. Sonoelasticity imaging: theory and experimental verification. *J Acoust Soc Am.* 1995;97(6):3875–3886.
32. Sanders JE, Goldstein BS, Leotla DF. Skin response to mechanical stress: adaptation rather than breakdown—a review of the literature. *J Rehabil Res Dev.* 1995;32(3):214–226.
33. Dora CD, DiMarco DS, Zobitz ME, Elliott DS. Time dependent variations in biomechanical properties of cadaveric fascia, porcine dermis, porcine small intestine submucosa, polypropylene mesh and autologous fascia in the rabbit model: implications for sling surgery. *J Urol.* 2004;171(5):1970–1973.
34. Edsberg LE. Microstructural evaluation of human skin subjected to static versus cyclic pressures. *J Rehabil Res Dev.* 2001;38(5):477–486.
35. Edsberg LE, Mates RE, Baier RE, Lauren M. Mechanical characteristics of human skin subjected to static versus cyclic normal pressures. *J Rehabil Res Dev.* 1999;36(2):133–141.
36. Lotta S, Scelsi R, Alfonsi E, et al. Morphometric and neurophysiological analysis of skeletal muscle in paraplegic patients with traumatic cord lesion. *Paraplegia.* 1991;29(4):247–252.
37. Martin TP, Stein RB, Hoepfner PH, Reid DC. Influence of electrical stimulation on the morphological and metabolic properties of paralyzed muscle. *J Appl Physiol.* 1992;72(4):1401–1406.
38. Round JM, Barr FM, Moffat B, Jones DA. Fibre areas and histochemical fibre types in the quadriceps muscle of paraplegic subjects. *J Neurol Sci.* 1993;116(2):207–211.
39. Scelsi R, Marchetti C, Poggi P, Lotta S, Lommi G. Muscle fiber type morphology and distribution in paraplegic patients with traumatic cord lesion. Histochemical and ultrastructural aspects of rectus femoris muscle. *Acta Neuropathol (Berl).* 1982;57(4):243–248.
40. Stilwill EW, Sahgal V. Histochemical and morphologic changes in skeletal muscle following cervical cord injury: a study of upper and lower motor neuron lesions. *Arch Phys Med Rehabil.* 1977;58(5):201–206.
41. Goldstein B, Sanders J. Skin response to repetitive mechanical stress: a new experimental model in pig. *Arch Phys Med Rehabil.* 1998;79(3):265–272.
42. Lieber RL, Friden JO, Hargens AR, Feringa ER. Long-term effects of spinal cord transection on fast and slow rat skeletal muscle. II. Morphometric properties. *Exp Neurol.* 1986;91(3):435–448.
43. Lieber RL, Johansson CB, Vahlsing HL, Hargens AR, Feringa ER. Long-term effects of spinal cord transection on fast and slow rat skeletal muscle. I. Contractile properties. *Exp Neurol.* 1986;91(3):423–434.
44. Sanders JE, Goldstein BS. Collagen fibril diameters increase and fibril densities decrease in skin subjected to repetitive compressive and shear stresses. *J Biomech.* 2001;34(12):1581–1587.
45. Klaesner JW, Hastings MK, Zou D, Lewis C, Mueller MJ. Plantar tissue stiffness in patients with diabetes mellitus and peripheral neuropathy. *Arch Phys Med Rehabil.* 2002;83(12):1796–1801.
46. Huang DT, Mak AF. A finite element analysis of indentation on a soft tissue layers—The effect of indenter misalignment and nonparallel tissue layer. *Proceedings of the International Conference on Biomedical Engineering;* 1994; Hong Kong, China. Pp. 397–400.
47. Zheng YP, Choi YKC, Wong K, Chan S, Mak AF. Biomechanical assessment of plantar foot tissue in diabetic patients using an ultrasound indentation system. *Ultrasound Med Biol.* 2000;26(3):451–456.
48. Zheng YP, Leung SF, Mak AF. Assessment of neck tissue fibrosis using an ultrasound palpation system: a feasibility study. *Med Biol Eng Comput.* 2000;38(5):497–502.
49. Zheng YP, Mak AF. Extraction of quasi-linear viscoelastic parameters for lower limb soft tissues from manual indentation experiment. *J Biomech Eng.* 1999;121(3):330–339.
50. Huang YP, Zheng YP, Leung SF. Quasi-linear viscoelastic properties of fibrotic neck tissues obtained from ultrasound indentation tests in vivo. *Clin Biomech.* 2005;20(2):145–154.
51. Lau JC, Li-Tsang CW, Zheng YP. Application of tissue ultrasound palpation system (TUPS) in objective scar evaluation. *Burns.* 2005;31(4):445–452.